

Autocrine laminin-5 ligates $\alpha 6\beta 4$ integrin and activates RAC and NF κ B to mediate anchorage-independent survival of mammary tumors

Nastaran Zahir,^{1,2} Johnathon N. Lakins,¹ Alan Russell,^{3,4} WenYu Ming,⁵ Chandrima Chatterjee,¹ Gabriela I. Rozenberg,¹ M. Peter Marinkovich,³ and Valerie M. Weaver^{1,2}

¹Department of Pathology and Laboratory Medicine, School of Medicine and ²Department of Bioengineering, Institute for Medicine and Engineering, University of Pennsylvania, Philadelphia, PA 19104

³Program in Epithelial Biology, Stanford University School of Medicine, Stanford, CA 94305

⁴Department of Cell Biology, Cytokinetics, Inc., South San Francisco, CA 94080

⁵Wells Center for Pediatrics Research, Indiana University School of Medicine, Indianapolis, IN 46202

Invasive carcinomas survive and evade apoptosis despite the absence of an exogenous basement membrane. How epithelial tumors acquire anchorage independence for survival remains poorly defined. Epithelial tumors often secrete abundant amounts of the extracellular matrix protein laminin 5 (LM-5) and frequently express $\alpha 6\beta 4$ integrin. Here, we show that autocrine LM-5 mediates anchorage-independent survival in breast tumors through ligation of a wild-type, but not a cytoplasmic tail-truncated $\alpha 6\beta 4$ integrin. $\alpha 6\beta 4$ integrin does not mediate tumor survival through activation of ERK or AKT. Instead, the cytoplasmic tail of $\beta 4$

integrin is necessary for basal and epidermal growth factor-induced RAC activity, and RAC mediates tumor survival. Indeed, a constitutively active RAC sustains the viability of mammary tumors lacking functional $\beta 1$ and $\beta 4$ integrin through activation of NF κ B, and overexpression of NF κ B p65 mediates anchorage-independent survival of nonmalignant mammary epithelial cells. Therefore, epithelial tumors could survive in the absence of exogenous basement membrane through autocrine LM-5- $\alpha 6\beta 4$ integrin-RAC-NF κ B signaling.

Introduction

Malignant transformation is linked to the migration of transformed epithelial cells across the endogenous basement membrane (BM) and their survival and proliferation in the surrounding interstitial collagen-rich stroma. Because normal mammary epithelial cells (MECs) require ligation of BM receptors to grow and survive (Weaver et al., 1997), invasive breast cancers must be able to resist apoptosis. Consistently, endogenous apoptosis rates decrease as MECs transition from ductal carcinoma in situ to invasive carcinoma (Gandhi et al., 1998), and immortalized mammary tumor cells frequently exhibit apoptosis resistance (Fernandez et al., 2002). However, how transformed MECs acquire apoptosis resistance remains poorly understood.

Address correspondence to Valerie M. Weaver, Institute for Medicine and Engineering, University of Pennsylvania, 1170 Vagelos Research Laboratory, 3340 Smith Walk, Philadelphia, PA 19104-6383. Tel.: (215) 573-7389. Fax: (215) 573-6815.

email: vmweaver@mail.med.upenn.edu

Key words: mammary epithelial cell; $\beta 4$ integrin; apoptosis; GTPase; microenvironment

Breast tumors and immortalized mammary tumor cells frequently lose expression of $\alpha 3\beta 1$ and $\alpha 2\beta 1$ integrins, which are the BM receptors that support normal MEC growth, differentiation, and survival (Weaver et al., 1996). Mammary tumors also express high amounts of antiapoptotic proteins such as activated focal adhesion kinase (Cance et al., 2000), NF κ B (Sovak et al., 1997), bcl-2 (Kalogeraki et al., 2002), and survivin (Tanaka et al., 2000), and often have elevated levels of active pro-survival kinases such as ERK, PI 3, and AKT (Fukazawa et al., 2002). Therefore, apoptosis-resistant breast tumors could arise through selection of MECs that express sufficient quantities of antiapoptotic molecules that permit growth and survival in the absence of adhesion (anoikis; Frisch and Ruoslahti, 1997).

Primary human breast tumors frequently synthesize and secrete ECM proteins such as fibronectin (Ioachim et al.,

Abbreviations used in this paper: 2D, two-dimensional; 3D, three-dimensional; $\beta 4\Delta$ cyto, tailless $\beta 4$ integrin; $\beta 4$ WT, wild-type $\beta 4$ integrin; BM, basement membrane; LM-5, laminin 5; MEC, mammary epithelial cell; rBM, reconstituted BM.

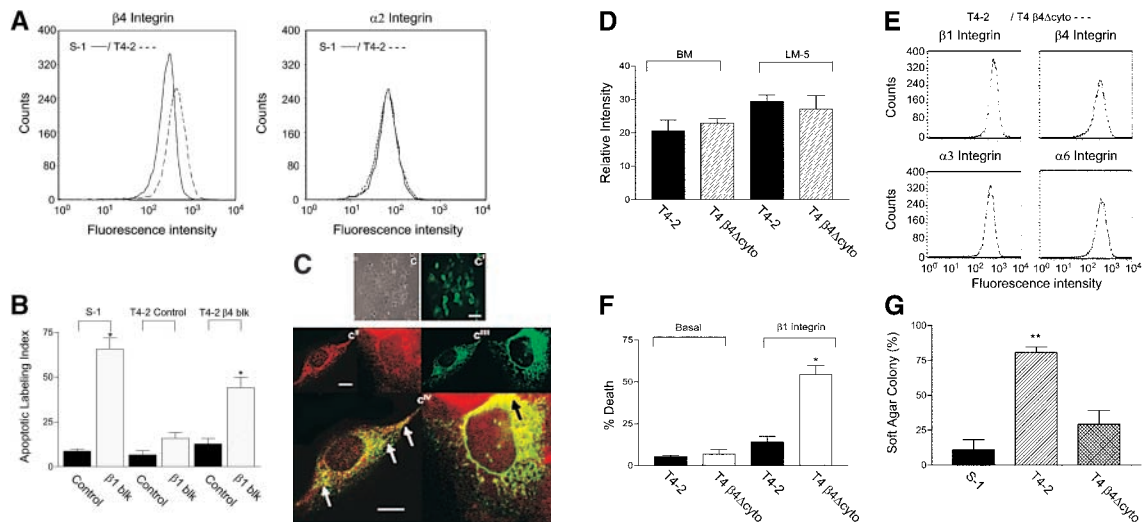


Figure 1. $\alpha 6 \beta 4$ integrin mediates anchorage-independent survival of mammary tumors. (A) FACS[®] analysis of cell surface integrin levels showing increased $\beta 4$ integrin in the T4-2s compared with S-1s (S-1, 265 vs. T4-2, 430) and similar amounts of $\alpha 2$ integrin. (B) Apoptotic labeling indices were calculated using the TUNEL assay in S-1s and T4-2s grown in rBM for 96 h in the presence of function-blocking mAb against $\beta 1$ integrin (A1B2) and/or $\beta 4$ integrin (ASC-3). Results are the mean \pm SEM of at least three separate experiments. (C) Phase-contrast (c), conventional immunofluorescence (EGFP; c') and confocal immunofluorescence microscopy of $\alpha 6$ integrin (Texas red; c''), $\beta 4$ integrin (EGFP; c'''), and $\alpha 6$ and $\beta 4$ integrin overlay (yellow; c^{iv}, as indicated by white and black arrows) showing uniform inducible expression of tailless EGFP $\beta 4$ integrin (T4 $\beta 4 \Delta cyto$) in T4-2s and clustering of $\alpha 6 / \beta 4 \Delta cyto$ integrin at membrane adhesion plaques. Bars: (c and c') 50 μ m; (c''–c^{iv}) 20 μ m. (D) Relative cell adhesion levels calculated using a fluorescence assay of control T4-2s (T4-2), and T4 $\beta 4 \Delta cyto$ cells showing comparable adhesion to rBM and LM-5 in both cell types. (E) FACS[®] analysis showing similar levels of the LM integrins $\beta 1$, $\beta 4$, $\alpha 3$, and $\alpha 6$ in T4-2 and T4 $\beta 4 \Delta cyto$ cells. (F) Cell viability was calculated using the Live/Dead assay for T4-2 or T4 $\beta 4 \Delta cyto$ cells grown in rBM for 96 h with or without a function-blocking mAb to $\beta 1$ integrin. (G) Soft agar assay results demonstrating that expression of the tailless $\beta 4$ integrin (T4 $\beta 4 \Delta cyto$) inhibits anchorage-independent growth of T4-2s, so that infected cells behave like S-1 nonmalignant cells (S-1). Results for B, D, F, and G are the mean \pm SEM of three to four separate experiments. (B and F) *, $P \leq 0.05$. (G) **, $P \leq 0.01$.

2002) and laminin-5 (LM-5; Davis et al., 2001). Malignant MECs often up-regulate $\alpha 5$ and αv integrins (Koukoulis et al., 1993; Pena et al., 1994) and retain $\alpha 6 \beta 4$ integrin expression (Davis et al., 2001). Ligation of $\alpha 5 \beta 1$ integrin by fibronectin (Nista et al., 1997) and $\alpha 6 \beta 4$ integrin by LM-5 (Bachelder et al., 1999) supports cell growth and survival. Thus, apoptosis-resistant mammary tumors could arise through increased growth and survival of MECs that possess enhanced autocrine ECM–integrin signaling, although such a possibility has yet to be investigated.

We have been studying the role of MEC–ECM interactions and apoptosis resistance in the pathogenesis of breast cancer using the HMT-3522 human tumor progression model (Weaver et al., 1996). Analogous to breast tumor progression in vivo, the early passage, nonmalignant cells in this series (S-1) require ligation of $\alpha 2 \beta 1$ or $\alpha 3 \beta 1$ integrin for their growth and survival, whereas their tumorigenic progeny (T4-2) are anchorage independent (Wang et al., 1998). Instead of dying, in the absence of $\beta 1$ integrin ligation, the T4-2s revert to form polarized tissue structures that resemble nonmalignant acini (Weaver et al., 1997). We demonstrated that $\alpha 6 \beta 4$ integrin can mediate apoptosis resistance to exogenous apoptotic stimuli in three-dimensional (3D) tissues irrespective of growth and malignancy status if MEC tissues are polarized (Weaver et al., 2002). Because invasive breast tumors typically lose polarized tissue architecture (acini, ductal) and tumors often metastasize as isolated cells, we asked whether $\alpha 6 \beta 4$ integrin might also support the survival of mammary tumor cells lacking polar tissue

structure, and if so, how. Here, we report that nonpolarized malignant MECs grown as 3D structures survive via $\alpha 6 \beta 4$ integrin, provided they synthesize and secrete sufficient quantities of LM-5 and activate RAC and NF κ B.

Results

$\alpha 6 \beta 4$ integrin mediates anchorage-independent survival of mammary tumors

$\alpha 6 \beta 4$ integrin drives tumor invasion and migration (Mercurio and Rabinovitz, 2001), and mediates apoptosis resistance in polarized MEC acini (Weaver et al., 2002), suggesting that tumors that express $\alpha 6 \beta 4$ integrin could metastasize and acquire multi-drug resistance, provided they are able to recapitulate tissue polarity. Because tumor invasion requires loss of tissue integrity, and survival of individual and isolated clusters of tumor cells dictates metastatic efficiency (Wong et al., 2001), we investigated whether $\alpha 6 \beta 4$ integrin could also support the growth and survival of isolated tumor cells or disorganized tumor cell clusters. We used S-1 (nonmalignant) and T4-2 (tumorigenic) MECs from the HMT-3522 human mammary tumor progression model and investigated whether anchorage independence of the T4-2s depends on $\alpha 6 \beta 4$ integrin.

We found that total and cell surface $\beta 1$ and $\beta 4$ integrin expression are higher in the T4-2s compared with S-1s, but that $\alpha 2$ integrin levels remain constant (Fig. 1 A and Fig. 3 A; Weaver et al., 1997). We also determined that although isolated S-1s require $\beta 1$ integrin ligation for growth and sur-

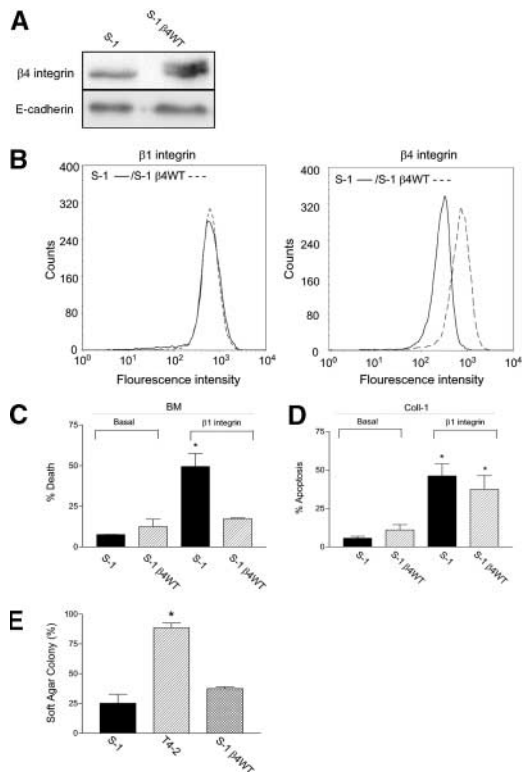


Figure 2. $\beta 4$ integrin overexpression does not induce anchorage-independent growth and survival of nonmalignant MECs. (A) Immunoblot analysis of total RIPA lysates for S-1 controls (S-1) and S-1 cells overexpressing a full-length $\beta 4$ integrin (S-1 $\beta 4$ WT) demonstrating increased expression of total $\beta 4$ integrin in S-1 $\beta 4$ WT cells. (B) FACS[®] analysis of membrane $\beta 1$ integrin and $\beta 4$ integrin in S-1s and S-1 $\beta 4$ WT showing elevated $\beta 4$ integrin expression in the infants (S-1, 260 vs. S-1 $\beta 4$ WT, 650) and no effect on $\beta 1$ integrin. (C) Cell viability was calculated using the Live/Dead assay for S-1 and S-1 $\beta 4$ WT grown in rBM for 96 h with and without a function-blocking mAb to $\beta 1$ integrin. (D) Percent apoptosis was calculated by scoring the number of caspase 3–positive cells for S-1 and S-1 $\beta 4$ WT grown in collagen I for 96 h with and without function-blocking mAb to $\beta 1$ integrin. (E) Soft agar assay results demonstrating that whereas malignant T4-2s exhibit anchorage independent growth and survival S-1s do not, even if they overexpress $\beta 4$ integrin (S-1 $\beta 4$ WT). Results for C–E are the mean \pm SEM of three to four separate experiments. *, $P \leq 0.05$.

vival, and T4-2s do not (Fig. 1 B), in the absence of both $\beta 1$ and $\beta 4$ integrin ligation, T4-2s die (Fig. 1 B). Thus, growth and survival of T4-2s require activation of either $\beta 4$ or $\beta 1$ integrin heterodimers.

Although much is known about how $\beta 1$ integrin heterodimers mediate cell viability, much less is known about how $\alpha 6\beta 4$ integrin directs cell survival. The cytoplasmic tail of $\beta 4$ integrin mediates proliferation through ras (Dans et al., 2001), invasion and survival via PI 3-kinase (Mercurio and Rabinovitz, 2001), and cell polarity via hemidesmosome formation (Weaver et al., 2002). To explore how $\alpha 6\beta 4$ integrin regulates MEC survival, we selected pooled populations of T4-2s that stably expressed high levels of a doxycyclin-repressible, EGFP-tagged, tail-less $\beta 4$ integrin ($\beta 4\Delta$ cyto; Fig. 1 C, c'), which colocalizes with $\alpha 6$ integrin at adhesion plaques (Fig. 1 C, c'', c''', and c^{IV}), equally supports adhesion to BM and purified

LM-5 when compared with wild-type $\beta 4$ integrin (T4-2 expressing $\beta 4$ WT; Fig. 1 D), and has no effect on plasma membrane levels of the LM integrins $\beta 1$, $\beta 4$, $\alpha 3$, and $\alpha 6$ (Fig. 1 E). We found that T4-2s expressing the EGFP-tagged $\beta 4\Delta$ cyto required $\beta 1$ integrin ligation for their survival (Fig. 1 F) and failed to form colonies in soft agar (Fig. 1 G). This indicates that $\alpha 6\beta 4$ integrin cytoplasmic function is required for the anchorage-independent survival phenotype of these tumors.

Increased $\beta 4$ integrin does not induce anchorage-independent survival of nonmalignant MECs

Because altering $\beta 4$ integrin activity had such a profound effect on tumor growth and survival, we asked whether overexpression of a $\beta 4$ WT would be sufficient to confer anchorage independence to nonmalignant MECs (S-1 cells). S-1 cells were infected with $\beta 4$ WT, and selected pooled populations of MECs expressing elevated levels of total (Fig. 2 A) and membrane-localized $\alpha 6\beta 4$ integrin (Fig. 2 B) were used for experiments. Control S-1s grown in 3D reconstituted BMs (rBMs) died rapidly when $\beta 1$ integrin–BM interactions were inhibited (Fig. 2 C; Weaver et al., 1997). However, S-1s overexpressing $\beta 4$ WT remained viable despite the absence of $\beta 1$ integrin–BM interactions (Fig. 2 C), indicating that increased activity of $\alpha 6\beta 4$ integrin can sustain the growth and survival of nonmalignant MECs. Yet, S-1s overexpressing $\beta 4$ WT died if $\beta 1$ integrin signaling was inhibited when viability experiments were conducted in 3D collagen I gels where exogenous LM ($\alpha 6\beta 4$ integrin ligand) was absent (Fig. 2 D). Moreover, S-1 $\beta 4$ WT MECs failed to grow in soft agar (Fig. 2 E, compare S-1 $\beta 4$ WT with S-1 control with T4-2). Therefore, a signal functionally linked to the cytoplasmic tail of ligated $\beta 4$ integrin supports the survival of isolated and nonpolarized clusters of nonmalignant MECs grown in 3D.

Autocrine LM-5 mediates $\beta 4$ integrin–dependent survival of mammary tumors

Breast tumors synthesize and secrete abundant quantities of LM-5 (Davis et al., 2001). Because we found that $\alpha 6\beta 4$ integrin supports anchorage independence of T4-2s but not of S-1s, we postulated that malignant transformation is either associated with constitutive activation of $\alpha 6\beta 4$ integrin or is linked to increased synthesis and secretion of autocrine LM-5. Consistent with the latter prediction, T4-2s have elevated levels of total $\beta 4$ integrin (Fig. 3 A) and plasma membrane $\beta 4$ integrin (Fig. 1 A), and synthesize and secrete more LM-5 than S-1s in 3D ECM gels (Fig. 3 B). Moreover, T4-2s colonies in soft agar are surrounded by copious amounts of LM-5 (Fig. 3 D), and when LM-5– $\alpha 6\beta 4$ integrin interactions and $\beta 1$ integrin ligation are simultaneously blocked (using function-blocking mAbs) in tumors embedded within a collagen I gel (in the absence of an exogenous $\alpha 6\beta 4$ integrin ligand), T4-2s die (Fig. 3 C). Consistently, although S-1s and S-1 $\beta 4$ WT cells embedded within 3D collagen I gels die when $\beta 1$ integrin ligation is inhibited, S-1 $\beta 4$ WT, but not control S-1s, grow and survive significantly better in the presence of exogenous purified LM-5 (Fig. 3

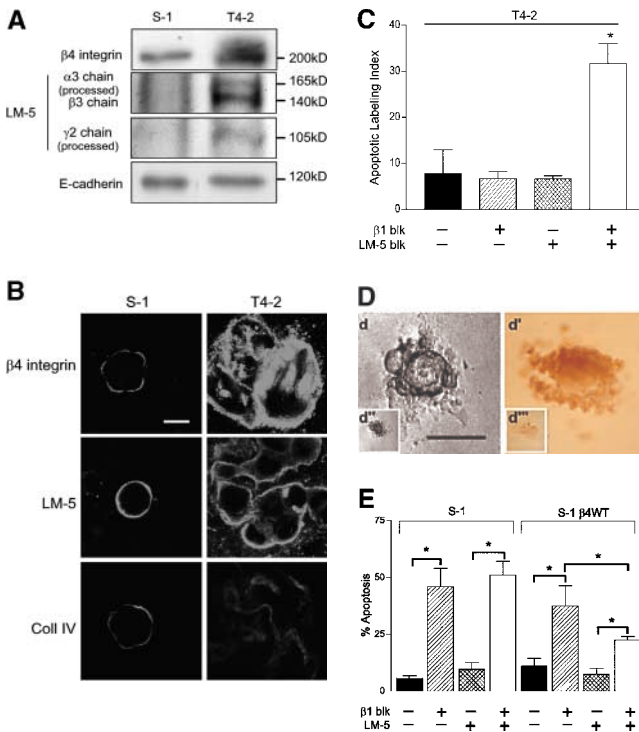


Figure 3. Autocrine LM-5 mediates anchorage-independent survival of mammary tumors. (A) Immunoblot analysis of total cell lysate and immunoprecipitants of secreted protein showing increased cellular $\beta 4$ integrin and secreted LM-5 in the T4-2s compared with S-1s. Note that E-cadherin levels remain constant regardless of the state of cell transformation. (B) Confocal Immunofluorescence microscopy images of $\beta 4$ integrin, LM-5, and collagen IV (Coll IV) in S-1 and T4-2 3D tissue structures. Data indicate that after malignant transformation, tumors have increased expression of cell surface $\beta 4$ integrin and secrete more extracellular LM-5, whereas collagen IV deposition does not change appreciably. All cultures were analyzed after 10 d inside the rBM. Bar, 20 μm . (C) Apoptotic labeling indices calculated using the TUNEL assay in T4-2s grown in collagen I for 96 h in the presence or absence of function-blocking mAb against $\beta 1$ integrin (A1IB2) and/or LM-5 (BM165). (D) Phase-contrast microscopy images of a representative T4-2 colony in soft agar (d) showing significant amounts of LM-5 deposition (d'; HRP) and specificity of staining in a parallel colony (d'') treated without primary mAb (d'''). Bar, 50 μm . (E) Percent apoptosis was calculated by scoring the number of caspase 3-positive S-1 and S-1 $\beta 4$ WT cells grown in collagen I for 96 h with or without 10 $\mu\text{g/ml}$ of exogenous LM-5 and/or function-blocking mAb to $\beta 1$ integrin. Results in C and E are the mean \pm SEM of at least three separate experiments. *, $P \leq 0.05$

D). Thus, tumors grow and survive in the absence of an exogenous BM if they synthesize and secrete sufficient quantities of LM-5 and up-regulate and ligate $\alpha 6\beta 4$ integrin.

$\alpha 6\beta 4$ integrin does not require ERK or AKT to mediate tumor survival

How does LM-5 ligation of $\alpha 6\beta 4$ integrin induce tumor survival? $\alpha 6\beta 4$ integrin can mediate the survival of tumor cells through activation of PI 3-kinase and AKT (Bachelder et al., 1999). Ligation of $\alpha 6\beta 4$ integrin also activates ERK via SHC-dependent activation of ras (Dans et al., 2001), and ERK supports anchorage-independent survival in epithelial cells (Howe et al., 2002). Although treatment with PD98059 effectively repressed ERK activity (Fig. 4 B), T4-2

survival remained unaffected, even when $\beta 1$ integrin ligation was simultaneously blocked (Fig. 4 A). Likewise, treatment of T4-2s with LY294002 inhibited AKT activity (Fig. 4 B), yet failed to compromise $\beta 1$ integrin-independent growth and survival (Fig. 4 A). Indeed, concomitant inhibition of ERK, PI 3-kinase, and $\beta 1$ integrin activity had no appreciable effect on tumor viability (Fig. 4 A).

Because AKT is an oncogene that can mediate adhesion-dependent survival in tumors (Hill and Hemmings, 2002), we directly tested the importance of AKT activity to $\alpha 6\beta 4$ integrin-dependent survival by expressing a dominant-negative K179M AKT. Despite stable expression of high levels of HA-tagged dominant-negative AKT (Fig. 4 D), T4-2s remained completely viable (Fig. 4 C) irrespective of their $\beta 1$ integrin ligation status, even when ERK activity was also inhibited (Fig. 4 C). Conversely, stable expression of the same dominant-negative AKT (Fig. 4 F) modestly but significantly compromised the viability of isolated S-1s embedded within rBM (Fig. 4 E). Consistently, stable overexpression of high levels of a constitutively active HA-tagged myristoylated AKT (Fig. 4 H, MyrAkt) only partially rescued S-1 survival when $\beta 1$ integrin ligation was blocked (Fig. 4 G), whereas overexpression and ligation of $\alpha 6\beta 4$ integrin was significantly more effective (Fig. 2 C). Thus, $\alpha 6\beta 4$ integrin must be able to support MEC survival through pathways that are distinct from AKT and ERK.

$\beta 4$ integrin mediates tumor survival through regulation of RAC

The Rho GTPase RAC is frequently overexpressed in tumors of the breast (Fritz et al., 1999), permits MEC growth in soft agar (Bouzahzah et al., 2001), and protects MDCK cells from anoikis (Coniglio et al., 2001). Because neither inhibition of AKT nor ERK kinase compromised T4-2 survival (Fig. 4, A–D), we asked whether $\alpha 6\beta 4$ integrin mediated T4-2 survival via activation of the Rho GTPase RAC. We assayed for RAC activity and determined that both basal and EGF-induced RAC activity significantly correlated with levels of expressed and ligated $\alpha 6\beta 4$ integrin. For example, T4-2s that express high $\alpha 6\beta 4$ integrin also have increased basal and EGF-induced RAC activity relative to S-1s (Fig. 5, A and B, compare specific activity of RAC in T4-2 with S-1; and Fig. 5, C and D, EGF-stimulated RAC activity). Moreover, ablating $\alpha 6\beta 4$ integrin function in the T4-2s by expressing the dominant-negative $\beta 4\Delta\text{cyto}$, reduced both basal (Fig. 5, A and B) and EGF-stimulated (Fig. 5 D) RAC activity, and overexpression of $\beta 4\text{WT}$ in the S-1 cells led to an increase in both basal (Fig. 5, A and B) and EGF-stimulated RAC activity (Fig. 5 C).

To determine whether $\alpha 6\beta 4$ integrin mediated anchorage-independent survival in T4-2s through RAC, we examined the survival phenotype of S-1 and T4-2s that expressed constitutively active and dominant-negative RhoGTPase mutants. Pooled populations of T4-2s stably expressing dominant-negative EGFP-N17 RAC (Fig. 6 A) had reduced RAC activity (unpublished data) and required $\beta 1$ integrin ligation for survival (Fig. 6 B), despite high levels of BM-ligated $\alpha 6\beta 4$ integrin (Figs. 1–3). S-1s that expressed low levels of endogenous $\beta 4$ integrin (Figs. 1–3) no longer depended on $\beta 1$ integrin activity for survival and were able to

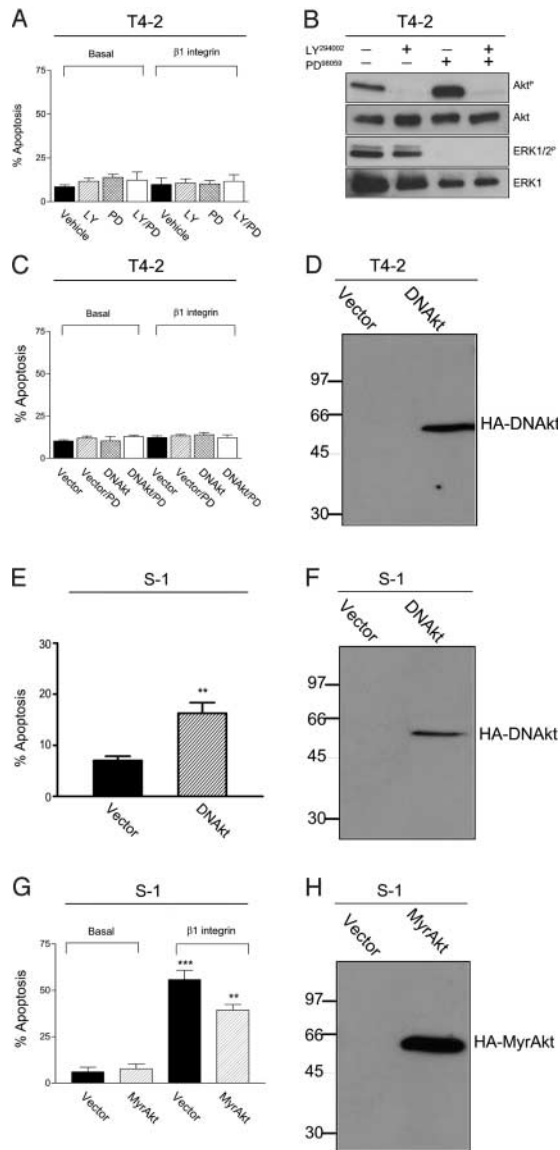


Figure 4. $\alpha 6\beta 4$ integrin does not mediate anchorage-independent survival in mammary tumors via ERK or AKT. (A) Percent apoptosis calculated by scoring the number of caspase 3–positive T4-2s grown in rBM for 96 h with or without a function-blocking mAb to $\beta 1$ integrin and treatment with 50 μ M of the PI 3-kinase inhibitor LY 294002 (LY), 20 μ M of the MEK inhibitor PD 98059 (PD), or vehicle (DMSO; Vehicle). (B) Immunoblot analysis of total and activated ERK and AKT in T4-2s grown in rBM with or without LY 294002 and/or PD 98059 treatment, as was described in A. (C) Percent apoptosis was calculated as described in A for T4-2 Vector control (Vector) and T4-2s expressing a dominant-negative AKT (DNAkt) grown in rBM for 96 h with or without a function-blocking mAb to $\beta 1$ integrin and treatment with the MEK inhibitor PD 98059 (PD) as indicated. (D) Immunoblot analysis of HA expressed in control T4-2s (Vector) and T4-2s expressing a HA-tagged dominant-negative AKT (DNAkt). (E) Percent apoptosis calculated as in A for S-1 control (Vector) and S-1s expressing a dominant-negative AKT (DNAkt) grown in rBM for 96 h. Note that expression of the dominant-negative AKT decreased survival of S-1s yet failed to compromise the viability of the T4-2s, even when $\beta 1$ integrin and ERK activity were inhibited. (F) Immunoblot analysis of HA in RIPA lysates of S-1 controls (Vector) and S-1s expressing an HA-tagged dominant-negative AKT (DNAkt). (G) Percent apoptosis was calculated as in A for S-1 vector control (Vector) and S-1s expressing a constitutively active myristoylated AKT (S1 MyrAkt) grown in rBM for 96 h with or without a function-blocking mAb to

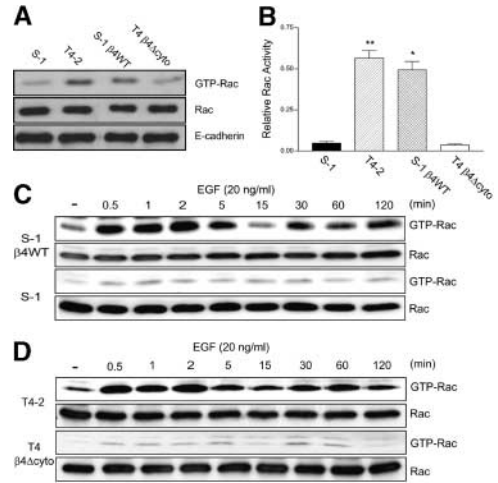


Figure 5. $\alpha 6\beta 4$ integrin regulates RAC activity in MECs. (A) Representative immunoblot of immunoprecipitated PAK-associated RAC (GTP-Rac), total cellular RAC (Rac) and total E-cadherin in S-1 control, T4-2 control, S-1s overexpressing $\beta 4$ integrin (S-1 $\beta 4$ WT), and T4-2s expressing a tailless $\beta 4$ integrin (T4 $\beta 4\Delta$ cyto). (B) Relative specific activity of RAC in S-1s, T4-2s, S-1 $\beta 4$ WT, and T4 $\beta 4\Delta$ cyto cells was calculated by densitometric analysis of immunoblots of activated (PAK-associated) RAC divided by total cellular RAC after normalization to total E-cadherin. Results are the mean \pm SEM of three to five separate experiments. *, $P \leq 0.05$; **, $P \leq 0.001$. (C) Time course of EGF-induced RAC activation, detected as described in A, in S-1s and S-1 $\beta 4$ WT cells. Data show significantly enhanced EGF-induced RAC activation in S-1s expressing higher levels of ligated $\beta 4$ integrin. (D) Time course of EGF-induced RAC activation, detected as described in A, in T4-2s and T4 $\beta 4\Delta$ cyto cells showing a significant reduction in EGF-induced RAC activation in T4-2s lacking the cytoplasmic tail of $\beta 4$ integrin. Time course results show one representative experiment out of four.

grow in soft agar (Fig. 6, F and G) if they stably expressed the constitutively active c-myc-V12 RAC (Fig. 6 E). Because T4-2s stably expressing a dominant-negative EGFP N19 Rho retained their apoptosis-resistant phenotype (Fig. 6, C and D), we suggest that LM-5–ligated $\alpha 6\beta 4$ integrin mediates mammary survival through RAC.

$\alpha 6\beta 4$ integrin mediates tumor survival via RAC-dependent activation of NF κ B

Having established a link between $\alpha 6\beta 4$ integrin, RAC, and survival, we next sought to delineate the mechanism whereby RAC mediates MEC survival. RAC can activate NF κ B p65 (Bouzahzah et al., 2001), and we showed that $\alpha 6\beta 4$ integrin induces apoptosis resistance in acini through NF κ B (Weaver et al., 2002). Upon investigation, we found that S-1s expressing c-myc-V12RAC had high amounts of nuclear NF κ B (Fig. 7, A and B) and that treating reverted T4-2 acini, which exhibit constitutively active NF κ B (Fig.

$\beta 1$ integrin. Data indicate that although active AKT does significantly enhance anchorage-independent survival of nonmalignant MECs, it does not completely rescue S-1 viability. (H) Immunoblot analysis of HA in S-1 controls (Vector) or S-1s expressing an HA-tagged constitutively active myristoylated AKT (MyrAkt). All apoptosis data are the mean \pm SEM of at least three separate experiments. **, $P \leq 0.01$; ***, $P \leq 0.001$.

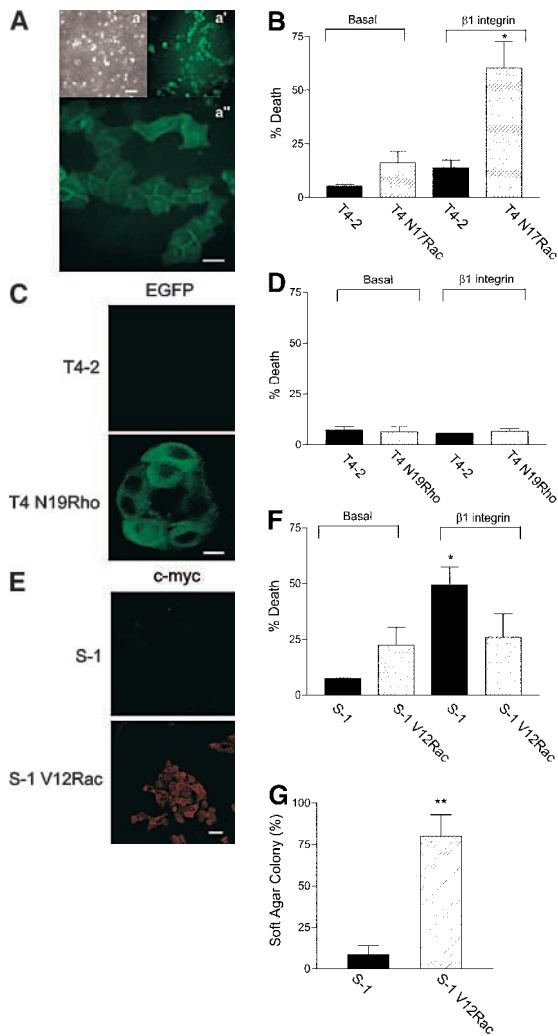


Figure 6. RAC mediates anchorage-independent survival in MECs. (A) Phase-contrast (a) and immunofluorescence microscopy images (EGFP; a' and a'') of low (a and a') and high (a'') magnifications of EGFP-tagged N17 RAC showing uniform high expression of the stable, exogenously expressed dominant-negative RAC protein in T4-2s. Bars: (a and a') 100 μm ; and (a'') 20 μm . (B) Cell viability calculated by the Live/Dead assay in control T4-2s (T4-2) and T4-2s expressing the N17 RAC (T4 N17Rac) grown in rBM for 96 h with or without a function-blocking mAb to $\beta 1$ integrin. (C) Immunofluorescence microscopy images of EGFP (FITC) detected only in T4-2s stably expressing EGFP N19Rho. Bar, 20 μm . (D) Cell viability calculated by the Live/Dead assay in control T4-2s (T4-2) and T4-2s expressing the N19Rho (T4N19Rho) grown in rBM for 96 h with or without a function-blocking mAb to $\beta 1$ integrin. (E) Immunofluorescence microscopy images of c-myc (Texas red) detected only in S-1s stably expressing a myc-tagged V12 RAC. Bar, 20 μm . (F) Cell viability calculated by the Live/Dead assay for S-1 controls (S-1) and S-1s expressing a c-myc-tagged V12 constitutively active RAC (S-1 V12Rac) grown in rBM for 96 h with or without a function-blocking mAb to $\beta 1$ integrin. (G) Soft agar assay results demonstrating that expression of exogenous V12RAC (S-1 V12Rac) renders nonmalignant S-1s (S-1) anchorage independent for growth and survival. Results shown in B, D, F, and G are mean \pm SEM of three experiments. *, $P \leq 0.05$; **, $P \leq 0.01$.

7, C and D; Weaver et al., 2002), with the Rho GTPase inhibitor Toxin A difficile repressed nuclear NF κ B significantly (Fig. 7, C and D, compare T4 β 1 with T4 β 1 Toxin A), inhibited RAC activity noticeably, disrupted actin orga-

nization appreciably, and eventually killed the T4-2 revertants (unpublished data). Because expressing a dominant-negative N19 Rho did not compromise the viability of T4-2 revertants (Fig. 6 D), whereas N17 RAC did (Fig. 6 B), we conclude that the Toxin A phenotype was likely due to inhibition of RAC.

Full-length $\beta 4$ integrin but not a $\beta 4\Delta\text{cyto}$ permits nuclear translocation (Fig. 7, E and F) and activation (Fig. 7 G) of NF κ B in T4-2s. Therefore, we predicted that if $\alpha 6\beta 4$ integrin regulates NF κ B activity via RAC, a constitutively active RAC (V12 RAC) should confer anchorage-independent survival to T4-2s expressing the $\beta 4\Delta\text{cyto}$, and tumor viability should depend on NF κ B activation. Consistently, T4-2s expressing both the $\beta 4\Delta\text{cyto}$ and a constitutively active RAC ($\beta 4\Delta\text{cyto}/\text{V12 RAC}$) survived when $\beta 1$ integrin–ECM interactions were blocked (Fig. 7 H), and tumor cells expressing both transgenes regained their ability to form colonies in soft agar (Fig. 7 I). Furthermore, anchorage-independent survival of the $\beta 4\Delta\text{cyto}/\text{V12RAC}$ -expressing T4-2s absolutely required NF κ B activity (Fig. 8 B). Indeed, T4-2s expressing only the $\beta 4\Delta\text{cyto}$ died when $\beta 1$ integrin function was blocked (Fig. 7 H and Fig. 1 F) and T4-2 $\beta 4\Delta\text{cyto}$ MECs failed to form colonies in soft agar (Fig. 7 I). Therefore, anchorage-independent growth and survival of T4-2s depends on a signaling pathway initiated through LM-5 ligation of $\alpha 6\beta 4$ integrin that is transduced by RAC and that depends on NF κ B activation.

NF κ B activity is necessary and sufficient for anchorage-independent survival of MECs

NF κ B is induced in the early stages of mammary involution and its activation is associated with enhanced MEC survival in culture (Clarkson et al., 2000). NF κ B expression and activity are increased in mammary tumors (Sovak et al., 1997). We have shown that NF κ B mediates resistance to chemotherapy, radiation treatment, and receptor-induced apoptosis (Baldwin, 2001; Weaver et al., 2002). To directly determine if $\alpha 6\beta 4$ integrin-dependent activation of NF κ B is essential for the survival of T4-2 revertants, we inhibited NF κ B nuclear translocation and assayed for effects on $\beta 1$ integrin–dependent survival. Incubation with the membrane-soluble peptide SN50 that specifically inhibits nuclear translocation of NF κ B, but not the nonfunctional peptide SN50M, induced apoptosis in the control T4-2 and T4 $\beta 4\Delta\text{cyto}/\text{V12RAC}$ revertants, but had no effect on viability when $\beta 1$ integrin was ligated (Fig. 8, A and B; unpublished data). Moreover, sequestering NF κ B in the cytosol through expression of a mutant I κ B α (I κ B α M) also rendered the T4-2s anchorage dependent for their survival (Fig. 8 C). Therefore, our data indicate that LM-5 ligation of $\alpha 6\beta 4$ integrin likely activates NF κ B via a RAC-dependent pathway that acts upstream of IKK α/β kinases. If true, then we reasoned that constitutive activation of NF κ B should render nonmalignant MECs anchorage independent for growth and survival. We addressed this possibility by assaying for integrin-dependent survival and anchorage-independent colony formation in S-1s that overexpressed NF κ B. Consistently, we found that expressing an exogenous NF κ B in S-1s led to constitutive nuclear localization of p65 (Fig. 8, D and E) and per-

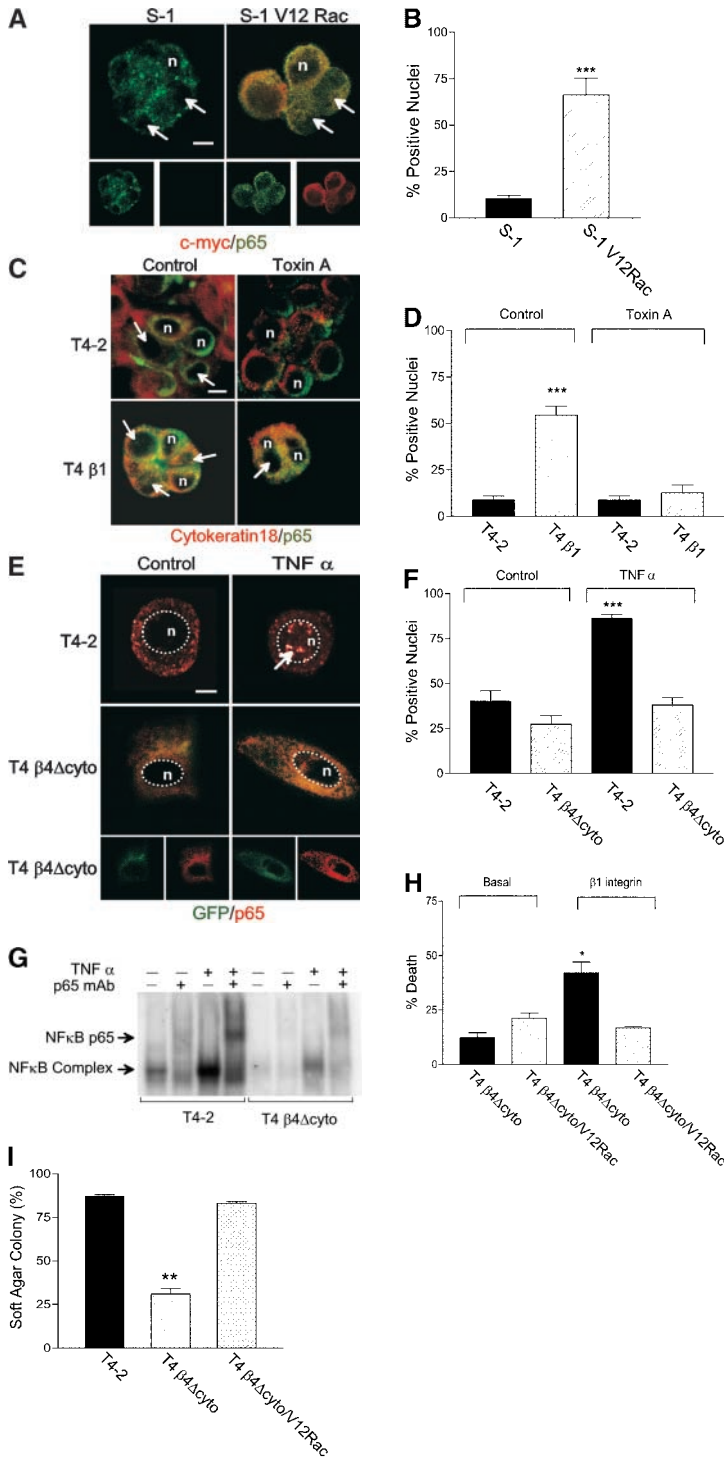


Figure 7. $\beta 4$ integrin activates NF κ B via RAC to mediate anchorage-independent survival in mammary tumors. (A) Confocal immunofluorescence microscopy images of c-myc (Texas red) and NF κ B p65 (FITC) of S-1 controls (S-1) and S-1 V12Rac expressing MECs (S-1 V12 Rac) grown in rBM for 8–10 d showing high levels of nuclear NF κ B p65 in the S-1 V12 Rac MECs (arrows, nuclei as indicated by “n”) and low to nondetectable amounts in the control S-1s (arrows). Bar, 20 μ m. (B) Quantification of 100–200 representative cells as shown in A, illustrating there is a significant increase in nuclear NF κ B p65 when RAC activity is elevated. (C) Confocal immunofluorescence microscopy images of cyto-keratin 18 (Texas red) and NF κ B p65 (FITC) of T4-2 controls (T4-2) and T4-2 revertants (T4 β 1) grown in rBM for 12 d and treated with or without the Rho GTPase inhibitor Toxin A (*C. difficile*; 200 ng/ml). Note the presence of detectable nuclear p65 in the T4 β 1 cells (arrows) and its absence in the Toxin A–treated structures. Bar, 20 μ m. (D) Quantification of 100–200 representative cells from similar images shown in C demonstrating high levels of nuclear NF κ B p65 in T4 β 1 structures that decrease significantly after treatment with Toxin A. (E) Confocal immunofluorescence microscopy images of NF κ B p65 (Texas red), EGFP protein (EGFP), and overlay of NF κ B p65 and EGFP protein (yellow) in T4-2 controls (T4-2) and T4-2s expressing an EGFP-tagged tailless $\beta 4$ integrin (T4 $\beta 4\Delta$ cyto). In the absence of a cytoplasmic $\beta 4$ integrin tail, tumors fail to activate NF κ B in response to TNF- α treatment, indicated by absence of staining in the nuclei (n) and presence of punctate staining in control nuclei (arrow). Bar, 20 μ m. (F) Quantification of 100–200 representative cells from similar images as shown in E illustrating a significant increase in nuclear NF κ B p65 only in T4-2s treated with TNF- α but not in T4 $\beta 4\Delta$ cyto cells. (G) Gel shift showing detectable binding of a transcriptional complex containing the NF κ B p65 protein (supershift), its significant enhancement after TNF- α treatment in T4-2s, and its absence in T4-2s lacking the cytoplasmic tail of the $\beta 4$ integrin (T4 $\beta 4\Delta$ cyto). (H) Cell viability calculated by the Live/Dead assay for T4 $\beta 4\Delta$ cyto cells and T4-2s expressing both the $\beta 4\Delta$ cyto and a constitutively active RAC (T4 $\beta 4\Delta$ cyto/V12Rac) grown in rBM for 96 h with and without a function-blocking mAb to $\beta 1$ integrin. (I) Soft agar assay results demonstrating that expression of exogenous V12RAC supports anchorage-independent growth and survival of T4 $\beta 4\Delta$ cyto cells. Results from B, D, F, H, and I are the mean \pm SEM of three to four experiments. *, $P \leq 0.05$; **, $P \leq 0.01$; and ***, $P \leq 0.001$.

mitted S-1s to form viable colonies in soft agar (Fig. 8 G) and to grow and survive in the absence of $\beta 1$ integrin ligation (Fig. 8 F). Thus, in the absence of ECM adhesion NF κ B can sustain MEC survival.

Discussion

We used paired nonmalignant (S-1) and tumor cells (T4-2) from the HMT-3522 tumor progression model and 3D agarose, collagen I, and rBM assays to investigate whether anchorage-independent growth and survival of mammary tu-

mors depends on autocrine LM-5 ligation of $\alpha 6\beta 4$ integrin. We found that malignant transformation is associated with up-regulation of $\alpha 6\beta 4$ integrin and increased LM-5 secretion, and that ligation of overexpressed full-length but not a $\beta 4\Delta$ cyto, in combination with autocrine LM-5, is necessary and sufficient to induce anchorage-independent growth and survival in MECs, even in the absence of a polar tissue structure. Our results are consistent with the idea that MECs that secrete sufficient quantities of LM-5 and retain $\alpha 6\beta 4$ integrin become selected during malignant transformation because they are able to grow and survive in the absence of exogenous

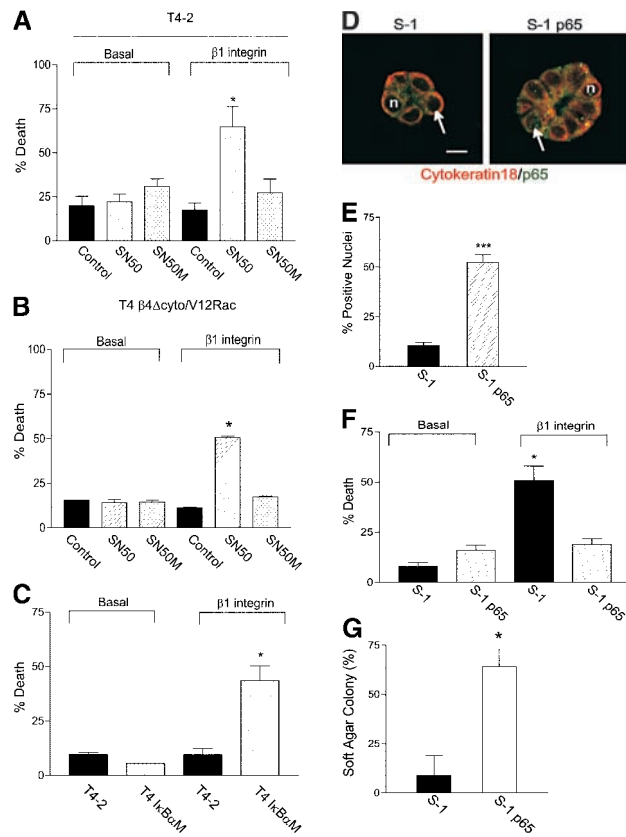


Figure 8. NFκB activation is necessary and sufficient for anchorage-independent survival of MECs. (A and B) Cell viability was calculated using the Live/Dead assay for T4-2s (A) and T4 β4Δ cyto/V12RAC (B) MECs treated with either vehicle (Control), a peptide that inhibits nuclear translocation of NFκB SN50 (SN50), or a nonfunction-blocking peptide SN50M (SN50M) grown in rBM for 96 h with or without a function-blocking mAb to β1 integrin. (C) Cell viability calculated using the Live/Dead assay for T4-2 controls (T4-2) or T4-2s expressing a mutant IκBα (IκBαM) grown and treated as in A. (D) Confocal immunofluorescence microscopy images of Cytokeratin 18 (Texas red) and NFκB p65 (FITC) in S-1 controls (S-1) and S-1s overexpressing an exogenous NFκB p65 (S-1 p65) showing constitutive nuclear NFκB p65 in the S-1 p65 structures (arrows, nuclei as indicated by "n"). Bar, 20 μm. (E) Quantification of 100–200 representative cells assayed from images similar to D demonstrating a significant increase in nuclear NFκB p65 in S-1s overexpressing NFκB p65 (S-1 p65). (F) Cell viability was calculated using the Live/Dead assay for S-1 and S-1 cells overexpressing NFκB p65 (S-1 p65) grown and treated as described for A. (G) Soft agar assay results demonstrating overexpressing exogenous NFκB p65 (S-1 p65) permits S-1s (S-1) to form colonies in soft agar. Results for A–C and E–G are the mean ± SEM of three to five experiments. *, $P \leq 0.05$; ***, $P \leq 0.001$.

BM cues. Because apoptosis limits metastatic efficiency (Wong et al., 2001), and LM-ligated β4 integrin also supports epithelial migration and invasion (Russell et al., 2003) and mediates immune and multi-drug resistance (Weaver et al., 2002), our results could explain why metastatic breast tumors frequently express β4 integrin (Menard et al., 1994) and why patients that express both BM protein and α6β4 integrin have the worst prognosis (Tagliabue et al., 1998).

α6β4 integrin can support tumor survival through PI 3- and AKT kinase (Bachelder et al., 1999) and keratinocyte proliferation through ERK (Dans et al., 2001), and β4 integrin can activate NFκB through AKT and ERK (Bozinovski

et al., 2002). Yet, we found that α6β4 integrin activates NFκB and mediates MEC survival through RAC, and not through AKT or ERK. One plausible explanation for the discrepancy between our results and those published by others is that we conducted our experiments in the context of 3D malleable gels. In contrast to cells grown as two-dimensional (2D) monolayers on rigid, planar substrates, cells embedded within 3D malleable gels more accurately recapitulate normal and malignant tissue organization and behavior (Jacks and Weinberg, 2002). For example, MECs grown to form tissuelike structures (acini) in 3D BM gels are able to differentiate and optimally synthesize β casein in response to lactogenic hormones (Roskelley et al., 1994). Likewise, salivary epithelial cells form acini that express cystatin only in the context of a 3D BM gel (Royce et al., 1993), and keratinocytes recapitulate epidermal differentiation, including filaggrin expression, most efficiently when grown as 3D organotypic rafts (Javaherian et al., 1998). Furthermore, MMP1 significantly enhances tumor growth in 3D, but has no effect on cell proliferation in 2D (Hotary et al., 2003); and RAC is required for cyst polarity in MDCKs grown within 3D collagen gels, but has no effect on MDCK polarity when cells are grown on 2D planar, rigid membranes (O'Brien et al., 2001). Why cells behave differently when grown on a planar, rigid substrate versus a 3D malleable gel remains an open question. What is known is that fibroblasts do not assemble focal adhesions containing αvβ3 integrin and activated focal adhesion kinase in response to a 3D ECM, but do so when plated on top of a 2D matrix (Cukierman et al., 2001). Moreover, MECs cultured on 2D planar substrates transiently activate MAP kinase in response to EGF, whereas MECs grown within 3D gels to form acini do not (Wang et al., 1998); and polarized mammary structures grown within 3D gels are recalcitrant to a diverse array of apoptotic stimuli, whereas MECs spread on a 2D planar substrate remain sensitive (Weaver et al., 2002; unpublished data). Thus the composition of integrin adhesions and integrin signaling function appear to be differentially regulated in 2D and 3D, implying that α6β4 integrin may regulate epithelial survival by different mechanisms in 2D and 3D.

The Rho GTPases, RAC and Rho, are overexpressed in tumors (Fritz et al., 1999), and RAC enhances tumor invasion in culture (Keely et al., 1997) and supports breast tumor metastasis in vivo (Bouzahzah et al., 2001). We found that in MECs, EGF stimulation of RAC depends almost entirely on LM ligation of a full-length α6β4 integrin. Likewise, we found that NFκB activation also requires functional α6β4 integrin. Because LM-5 and α6β4 integrin are so often retained in primary breast tumors (Tagliabue et al., 1998; Davis et al., 2001), our results offer a plausible explanation for why RAC and NFκB activity are frequently elevated in these same malignant tissues (Sovak et al., 1997; Fritz et al., 1999). Moreover, by establishing a functional link between RAC and NFκB in 3D tissues, our findings could explain how RAC supports mammary tumor growth in soft agar (Bouzahzah et al., 2001) and why RAC supports the viability of cells actively migrating into 3D collagen gels (Cho and Klemke, 2000). Finally, our data predict that α6β4 integrin could drive tumor metastasis through an alternative PI 3-kinase and Akt-independent mechanism (Mercurio and Rabinovitz, 2001).

Current theory maintains that anoikis is circumvented early during malignant transformation (Frisch and Ruoslahti, 1997) and that metastatic cells are selected thereafter from the invasive tumor population through pressures exerted by the tumor tissue microenvironment (Wouters et al., 2003). Yet, tumor metastasis can occur early during cancer (Wasserberg et al., 2002); metastatic cells have been found in the bone marrow of patients with early stage tumors (Menard et al., 1994), and tumor cells do circulate in the blood of patients with benign disease (Hardingham et al., 2000). Metastatic tumors frequently express integrins such as αv , $\alpha 5$, $\alpha 6$, and $\beta 4$, and often secrete ECM proteins including collagen IV, LM-5, and fibronectin (Davis et al., 2001; Ioachim et al., 2002). Tumor metastasis and extravasation are facilitated by integrin–ECM interactions (Clezzardin, 1998). Therefore, it is plausible that apoptosis-resistant metastatic tumors arise early during malignancy through selection of transformed cells that express ECM proteins and retain integrins that support migration, invasion, and survival. Because we show that malignant transformation is linked to autocrine LM-5, that LM-5 supports cell survival by inducing $\alpha 6\beta 4$ integrin–RAC–NF κ B signaling, and that LM-5–ligated $\alpha 6\beta 4$ integrin and RAC support epithelial motility and invasion (Russell et al., 2003), our data underscore the feasibility of this concept.

Materials and methods

Materials

We used commercial EHS matrix (Matrigel; Collaborative Research) for the rBM assays; Vitrogen 100 (bovine skin collagen I; Celtrix Laboratories), 3 mg/ml and 10 μ g/ml of affinity-purified LM-5 (Russell et al., 2003) for coating culture dishes; and 0.3% Cellagen Solution AC-5 (ICN Biomedicals) for the 3D collagen I assays. Primary antibodies were as follows: LM-5, rabbit sera pKa1, and clone BM165 (Russell et al., 2003); $\alpha 6$ integrin, clone GoH3 (BD Biosciences); $\beta 1$ integrin, clones A1B2 (provided by C. Damsky, University of California, San Francisco, San Francisco, CA), and TS2/16 (ATCC); $\beta 4$ integrin, rabbit sera, and clones 3E1, ASC-3, and ASC-8; and $\alpha 2$ integrin, clone 10G11 (all from Chemicon International); $\text{I}\kappa\text{B}\alpha$ /MAD-3, clone 25, and NF κ B p65, rabbit sera (Santa Cruz Biotechnology, Inc.) and clone 20 (BD Biosciences); cytokeratin 18, clone RCK106 (BD Biosciences); RAC1, clone 102 (BD Biosciences); c-myc, clone 9E10 (Oncogene Research Products), and AKT and Phospho-ser472/473/474-AKT; ERK1, rabbit sera (BD Biosciences), phosphoERK1/2 (Thr202/Tyr204), rabbit sera (New England BioLabs, Inc.); activated caspase 3, rabbit sera (Cell Signaling), and HA.11, clone 16B12 (Babco). Secondary antibodies were as follows: horseradish peroxidase, and biotinylated mouse IgG (Vector Laboratories); FITC, and Texas red–conjugated and nonconjugated anti-mouse, anti-rat, and anti-rabbit goat polyclonal antibodies and nonspecific rat and mouse IgGs (Jackson ImmunoResearch Laboratories). Reagents were as follows: NF κ B SN50, active cell-permeable inhibitor peptide (50 μ M in PBS), NF κ B SN50M, inactive cell-permeable control peptide (50 μ M in PBS); the EGFR-specific tyrosine kinase inhibitor Tyrphostin AG 1478 (160 μ M in DMSO), and the Rho GTPase inhibitor toxin A *Clostridium difficile* (10 mM in DMSO; Calbiochem); the MEK1 inhibitor PD98059 (50 μ M in DMSO); and the PI 3-kinase inhibitor LY 294002 (50 μ M in ethanol; BIOMOL Research Laboratories, Inc.).

Cell culture

The HMT-3522 MECs were grown in 2D and embedded ($0.5\text{--}0.8 \times 10^6$ cells/ml) within ECM gels and phenotypic reversion of T4-2s using $\beta 1$ integrin mAb A1B2 or Tyrphostin AG 1478 as described previously (Wang et al., 1998).

Adhesion assay

Cell adhesion was assessed using a fluorescence attachment assay. In brief, plates coated with LM-5 or rBM (100 μ g/ml) were blocked (1 h; 0.1% BSA), incubated (60 min, 37°C), washed (3 \times PBS), incubated with 4

μ M calcein (20 min, RT), and quantified using a fluorescence plate reader (model Fluoroskan Ascent FI; LabSystems).

Anchorage-independent assay

Anchorage-independent growth was assessed using a soft agar assay (Wang et al., 1998). In brief, 20,000 cells were plated in 1 ml DME/Ham's F12 containing 0.7% agarose, overlaid with 1 ml of 1% agarose, and 40- μ m colonies were scored positive after 21 d.

Function-blocking studies

To inhibit integrin function or LM-5 binding, cells were incubated with mAbs against $\beta 1$ integrin, clone A1B2 (1:25–1:100 ascites/ml ECM); $\beta 4$ integrin, clones ASC-3 or ASC-8 (4–16 μ g IgG/ml ECM); LM-5, clone BM165 (10 μ g IgG/ml ECM); or IgG isotype-matched control mAb (4–16 μ g IgG/ml ECM) at the time of embedment. To inhibit NF κ B nuclear translocation, the active inhibitor NF κ B SN50 or the inactive analogue NF κ B SN50M was added directly to the media.

Immunofluorescence analysis

Cells were directly fixed using 2–4% PFA or 100% methanol, and samples were incubated with primary mAbs, followed by either FITC- or Texas red–conjugated secondary antibodies. Nuclei were counterstained with DAPI (Sigma-Aldrich). Cells were either visualized using a scanning confocal laser (model 2000-MP; Bio-Rad Laboratories) attached to a fluorescence microscope (model Eclipse TE-300 [Nikon] or model MDIRBE [Leica]). Confocal images were recorded at 120 \times and conventional images were recorded at 40–60 \times .

Apoptosis assay

Apoptosis was assayed by the Live/Dead Assay (Molecular Probes) or by detection of internucleosomal DNA fragmentation in fixed cells using an in situ TUNEL assay (Boehringer) or via immunodetection of activated caspase 3. Percent death was calculated as cells positive for ethidium bromide expressed as a percentage of the total number of live cells scored positive by calcein staining (FITC). The apoptotic labeling index was calculated as the percentage of total cells positive for FITC-labeled 3'OH DNA ends, and percent apoptosis was determined as the percentage of total cells positive for activated caspase 3. The minimum number of cells scored was 200–400 per experimental condition. Cell death by apoptosis was confirmed by showing that DNA cleavage or caspase 3 activity could be inhibited by prior treatment with the caspase inhibitors YVAD CHO or DEVD-CHO (1 μ M; BIOMOL Research Laboratories, Inc.).

cDNA constructs

Full-length $\beta 4$ pRK-5 (provided by F. Giancotti, Memorial Sloan-Kettering Cancer Center, New York, NY) was used directly. The 2,710-bp EcoRI–BglII fragment from the $\beta 4$ pRK-5 construct was ligated with the EcoRI–BamHI vector fragment of pEGFP-N2, and an EcoRI–NotI fragment containing the $\beta 4$ integrin EGFP fusion was subcloned into an EcoRI–NotI vector fragment of Hermes HRS puro-GUS (provided by H. Blau, Stanford Medical Center, Stanford, CA). Myc-tagged V12RAC1 (provided by A. Hall, University College, London, UK) was cloned as an EcoRI fragment into LZRS-IRES-blasticidin; and N17RAC1 and N19RhoA (provided by E. Butcher, Stanford Medical Center) were cloned into the EGFP fusion vector EGFP-C1 (CLONTECH Laboratories, Inc.), and excised and recloned into LZRS-IRES-blasticidin by PCR using the EcoRI tailed primer GTPaseF, 5'. $\text{I}\kappa\text{B}\alpha$ and p65 cloned into PLZRS (provided by P. Khavari, Stanford Medical Center) were used directly. The BglII–BamHI fragment containing HA-tagged dominant-negative AKT (K179M) and the HindIII–EcoRI fragment containing the myristoylated HA-tagged AKT (provided by P. Tsichlis, Tufts University, Boston, MA) were subcloned into pLZRS.

Gene expression manipulations

Amphotropic retrovirus was produced in either modified 293 cells or in Phoenix amphi cells (provided by G. Nolan, Stanford Medical Center), and MECs were spin infected and selected using blasticidin. MECs were transfected with full-length $\beta 4$ pRK-5 and pcDNA 3.1 plasmid vector DNA or vector plasmid alone using LipofectAMINE (GIBCO BRL), and selected using G418. S-1 $\beta 4$ pRK-5–transfected cells were enriched for increased membrane localized $\beta 4$ integrin through differential adhesion to LM-5, and increased $\beta 4$ integrin levels were verified by FACS[®] analysis.

Electrophoretic mobility shift assay

To prepare nuclear extracts, cells were washed (1 \times PBS) and homogenized in nuclear isolation buffer (10 mM Hepes, pH 7.9, 10 mM KCl, 1

mM EDTA, 1 mM EGTA, 1 mM DTT, and 1 mM Pefabloc SC) with an addition of IGEPAI to 0.5%. After incubation (10 min, 4°C), nuclei were isolated by centrifugation (1 min, 14,000 rpm, 4°C) and nuclear extracts were prepared by homogenization and incubation in nuclear extraction buffer (20 mM Hepes, pH 7.9, 420 mM KCl, 1.5 mM MgCl₂, 20% glycerol, 0.5 mM DTT, 1 mM Pefabloc SC, and 10 µg/ml leupeptin), followed by centrifugation (15 min, 14,000 rpm, 4°C). Equal amounts of nuclear protein were used in the EMSA reaction with the NFκB consensus oligonucleotide sequence (5'-AGT TGA GGG GAC TTT CCC AGG C-3'). ³²P-Labeled oligonucleotide (150,000 cpm) was incubated with 5 µg of nuclear extract and gel shift binding buffer (10 min, RT; Promega Gel Shift Assay System). p65 rabbit antisera were added after the binding reaction, and the mixture was reincubated (20 min, RT). Specificity of binding was tested using competition analyses in which 10-fold molar excess of nonlabeled oligonucleotide sequence was added to a binding reaction. Complexes were resolved in 4.5% polyacrylamide gels (TE buffer: 90 mM Tris, 90 mM boric acid, and 2 mM EDTA, pH 8.0).

Flow cytometry

Cells were isolated, nonspecific binding was blocked (60 min Dulbecco's PBS, 0.1% BSA) and incubated with saturating concentrations of primary mAb (1 h), washed three times with Dulbecco's PBS, and labeled with FITC-conjugated goat immunoglobulin. Stained cells were washed three times with Dulbecco's PBS and immediately analyzed on a FACScan™ (Becton Dickinson). All manipulations were conducted at 4°C.

Immunoblot analysis

Cells were lysed (RIPA buffer: 50 mM Tris-HCl, pH 7.4, 150 mM sodium chloride, 1% NP-40, 0.5% deoxycholate, 0.2% SDS containing 20 mM sodium fluoride, and 1 mM sodium orthovanadate, and a cocktail of protease inhibitors), and equal amounts of protein were separated on reducing SDS-PAGE gels, immunoblotted, and detected with an ECL-Plus system (Amersham Biosciences). To assay for differences in total secreted LM-5, LM-5 was immunoprecipitated from conditioned media, and protein from equal cells was separated on SDS-polyacrylamide gels, immunoblotted, and detected as above.

RAC activation

Cells were treated with vehicle or 20 ng/ml EGF and incubated for indicated times, washed (2× PBS), and extracted (G protein buffer: 25 mM Hepes, pH 7.5, 150 mM NaCl, 1% Igepal CA-630, 10 mM MgCl₂, 1 mM EDTA, 10% glycerol, 1 mM Pefabloc SC, 10 µg/ml leupeptin, 10 µg/ml aprotinin, 1 mM sodium orthovanadate, and 1 mM sodium fluoride; 5–10 min). Lysates were centrifuged (10 min, 14,000 rpm), and supernatants were mixed with GST-PBD and incubated with glutathione-Sepharose beads (Amersham Biosciences; 60 min). Lysates were washed (3× lysis buffer), and bound protein was eluted with Laemmli buffer and separated on a 12% SDS-polyacrylamide gel. Active RAC was detected by immunoblotting with anti-RAC antibody, and specific activity was calculated by normalizing densitometric values of PAK-associated RAC to total RAC and E-cadherin. Purified GST-PBD, encoding amino acids 70–117 of PAK1, fused to GST (provided by J. Chernoff, Fox Chase Cancer Center, Philadelphia, PA).

We thank C. Damsky for the AIB2 mAb; Drs. P. Khavari, P. Tsichlis, A. Hall, E. Butcher, and F. Giancotti for cDNA clones; J. Chernoff for GST human PAK1 cDNA; G. Nolan for the Phoenix ampho cells; and Z. Werb and N. Boudreau for helpful comments.

This work was supported by National Cancer Institute grant CA 78731 and Department of Defense grant DAMD17-01-1-0368 to V.M. Weaver and grant DAMD17-01-1-0367 to J.N. Lakins; National Institutes of Health (NIH) grant P01 AR44-012 to A. Russell and A.P. Marinkovich; and NIH grant T32 HL07954-03 to N. Zahir.

Submitted: 5 February 2003

Accepted: 27 October 2003

References

Bachelder, R.E., M.J. Ribick, A. Marchetti, R. Falcioni, S. Soddu, K.R. Davis, and A.M. Mercurio. 1999. p53 inhibits α6β4 integrin survival signaling by promoting the caspase 3-dependent cleavage of AKT/PKB. *J. Cell Biol.* 147: 1063–1072.

Baldwin, A.S. 2001. Control of oncogenesis and cancer therapy resistance by the transcription factor NF-κappaB. *J. Clin. Invest.* 107:241–246.

Bouzahzah, B., C. Albanese, F. Ahmed, F. Pixley, M.P. Lisanti, J.D. Segall, J. Condeelis, D. Joyce, A. Minden, C.J. Der, et al. 2001. Rho family GTPases regulate mammary epithelium cell growth and metastasis through distinguishable pathways. *Mol. Med.* 7:816–830.

Bozinovski, S., J.E. Jones, R. Vlahos, J.A. Hamilton, and G.P. Anderson. 2002. Granulocyte/macrophage-colony-stimulating factor (GM-CSF) regulates lung innate immunity to lipopolysaccharide through Akt/Erk activation of NFκappa B and AP-1 in vivo. *J. Biol. Chem.* 277:42808–42814.

Cance, W.G., J.E. Harris, M.V. Iacocca, E. Roche, X. Yang, J. Chang, S. Simkins, and L. Xu. 2000. Immunohistochemical analyses of focal adhesion kinase expression in benign and malignant human breast and colon tissues: correlation with preinvasive and invasive phenotypes. *Clin. Cancer Res.* 6:2417–2423.

Cho, S.Y., and R.L. Klemke. 2000. Extracellular-regulated kinase activation and CAS/Erk coupling regulate cell migration and suppress apoptosis during invasion of the extracellular matrix. *J. Cell Biol.* 149:223–236.

Clarkson, R.W., J.L. Heeley, R. Chapman, F. Aillet, R.T. Hay, A. Wyllie, and C.J. Watson. 2000. NF-κappaB inhibits apoptosis in murine mammary epithelia. *J. Biol. Chem.* 275:12737–12742.

Clezardin, P. 1998. Recent insights into the role of integrins in cancer metastasis. *Cell. Mol. Life Sci.* 54:541–548.

Coniglio, S.J., T.S. Jou, and M. Symons. 2001. Rac1 protects epithelial cells against anoikis. *J. Biol. Chem.* 276:28113–28120.

Cukierman, E., R. Pankov, D.R. Stevens, and K.M. Yamada. 2001. Taking cell-matrix adhesions to the third dimension. *Science.* 294:1708–1712.

Dans, M., L. Gagnoux-Palacios, P. Blaikie, S. Klein, A. Mariotti, and F.G. Giancotti. 2001. Tyrosine phosphorylation of the beta 4 integrin cytoplasmic domain mediates Shc signaling to extracellular signal-regulated kinase and antagonizes formation of hemidesmosomes. *J. Biol. Chem.* 276:1494–1502.

Davis, T.L., A.E. Cress, B.L. Dalkin, and R.B. Nagle. 2001. Unique expression pattern of the alpha6beta4 integrin and laminin-5 in human prostate carcinoma. *Prostate.* 46:240–248.

Fernandez, Y., B. Gu, A. Martinez, A. Torregrosa, and A. Sierra. 2002. Inhibition of apoptosis in human breast cancer cells: role in tumor progression to the metastatic state. *Int. J. Cancer.* 101:317–326.

Frisch, S.M., and E. Ruoslahti. 1997. Integrins and anoikis. *Curr. Opin. Cell Biol.* 9:701–706.

Fritz, G., I. Just, and B. Kaina. 1999. Rho GTPases are over-expressed in human tumors. *Int. J. Cancer.* 81:682–687.

Fukazawa, H., K. Noguchi, Y. Murakami, and Y. Uehara. 2002. Mitogen-activated protein/extracellular signal-regulated kinase (MEK) inhibitors restore anoikis sensitivity in human breast cancer cell lines with a constitutively activated extracellular-regulated kinase (ERK) pathway. *Mol. Cancer Ther.* 1:303–309.

Gandhi, A., P.A. Holland, W.F. Knox, C.S. Potten, and N.J. Bundred. 1998. Evidence of significant apoptosis in poorly differentiated ductal carcinoma in situ of the breast. *Br. J. Cancer.* 78:788–794.

Hardingham, J.E., P.J. Hewett, R.E. Sage, J.L. Finch, J.D. Nuttall, D. Kotasek, and A. Dobrovic. 2000. Molecular detection of blood-borne epithelial cells in colorectal cancer patients and in patients with benign bowel disease. *Int. J. Cancer.* 89:8–13.

Hill, M.M., and B.A. Hemmings. 2002. Inhibition of protein kinase B/Akt. Implications for cancer therapy. *Pharmacol. Ther.* 93:243–251.

Hotary, K.B., E.D. Allen, P.C. Brooks, N.S. Datta, M.W. Long, and S.J. Weiss. 2003. Membrane type I matrix metalloproteinase usurps tumor growth control imposed by the three-dimensional extracellular matrix. *Cell.* 114:33–45.

Howe, A.K., A.E. Aplin, and R.L. Juliano. 2002. Anchorage-dependent ERK signaling—mechanisms and consequences. *Curr. Opin. Genet. Dev.* 12:30–35.

Ioachim, E., A. Charchanti, E. Briassoulis, V. Karavasilis, H. Tsanou, D.L. Arvanitis, N.J. Agnantis, and N. Pavlidis. 2002. Immunohistochemical expression of extracellular matrix components tenascin, fibronectin, collagen type IV and laminin in breast cancer: their prognostic value and role in tumour invasion and progression. *Eur. J. Cancer.* 38:2362–2370.

Jacks, T., and R.A. Weinberg. 2002. Taking the study of cancer cell survival to a new dimension. *Cell.* 111:923–925.

Javaherian, A., M. Vaccariello, N.E. Fusenig, and J.A. Garlick. 1998. Normal keratinocytes suppress early stages of neoplastic progression in stratified epithelium. *Cancer Res.* 58:2200–2208.

Kalogeraki, A., F. Garbagnati, M. Santinami, and O. Zoras. 2002. Proliferative activity (Ki-67), WT p53, Bcl-2 expression and their relationship to the tumor grade, in invasive ductal breast carcinomas. *In Vivo.* 16:141–144.

Keely, P.J., J.K. Westwick, I.P. Whitehead, C.J. Der, and L.V. Parise. 1997. Cdc42 and Rac1 induce integrin-mediated cell motility and invasiveness

- through PI(3)K. *Nature*. 390:632–636.
- Koukoulis, G.K., A.A. Howedy, M. Korhonen, I. Virtanen, and V.E. Gould. 1993. Distribution of tenascin, cellular fibronectins and integrins in the normal, hyperplastic and neoplastic breast. *J. Submicrosc. Cytol. Pathol.* 25:285–295.
- Menard, S., P. Squicciarini, A. Luini, V. Sacchini, D. Rovini, E. Tagliabue, P. Veronesi, B. Salvadori, U. Veronesi, and M.I. Colnaghi. 1994. Immunodetection of bone marrow micrometastases in breast carcinoma patients and its correlation with primary tumour prognostic features. *Br. J. Cancer*. 69: 1126–1129.
- Mercurio, A.M., and I. Rabinovitz. 2001. Towards a mechanistic understanding of tumor invasion—lessons from the $\alpha 6\beta 4$ integrin. *Semin. Cancer Biol.* 11:129–141.
- Nista, A., C. Leonetti, G. Bernardini, M. Mattioni, and A. Santoni. 1997. Functional role of $\alpha 4\beta 1$ and $\alpha 5\beta 1$ integrin fibronectin receptors expressed on adriamycin-resistant MCF-7 human mammary carcinoma cells. *Int. J. Cancer*. 72:133–141.
- O'Brien, L.E., T.S. Jou, A.L. Pollack, Q. Zhang, S.H. Hansen, P. Yurchenco, and K.E. Mostov. 2001. Rac1 orientates epithelial apical polarity through effects on basolateral laminin assembly. *Nat. Cell Biol.* 3:831–838.
- Pena, L., A. Nieto, M.D. Perez Alenza, A. Rodriguez, M.A. Sanchez, and M. Castano. 1994. Expression of fibronectin and its integrin receptor $\alpha 5\beta 1$ in canine mammary tumours. *Res. Vet. Sci.* 57:358–364.
- Roskelley, C.D., P.Y. Desprez, and M.J. Bissell. 1994. Extracellular matrix-dependent tissue-specific gene expression in mammary epithelial cells requires both physical and biochemical signal transduction. *Proc. Natl. Acad. Sci. USA*. 91:12378–12382.
- Royce, L.S., M.C. Kibbey, P. Mertz, H.K. Kleinman, and B.J. Baum. 1993. Human neoplastic submandibular intercalated duct cells express an acinar phenotype when cultured on a basement membrane matrix. *Differentiation*. 52: 247–255.
- Russell, A.J., E.F. Fincher, L. Millman, R. Smith, V. Vela, E.A. Waterman, C.N. Dey, S. Guide, V.M. Weaver, and M.P. Marinkovich. 2003. $\alpha 6\beta 4$ integrin regulates keratinocyte chemotaxis through differential GTPase activation and antagonism of $\alpha 3\beta 1$ integrin. *J. Cell Sci.* 116:3543–3556.
- Sovak, M.A., R.E. Bellas, D.W. Kim, G.J. Zanieski, A.E. Rogers, A.M. Traish, and G.E. Sonenshein. 1997. Aberrant nuclear factor- κ B/Rel expression and the pathogenesis of breast cancer. *J. Clin. Invest.* 100:2952–2960.
- Tagliabue, E., C. Ghirelli, P. Squicciarini, P. Aiello, M.I. Colnaghi, and S. Menard. 1998. Prognostic value of $\alpha 6\beta 4$ integrin expression in breast carcinomas is affected by laminin production from tumor cells. *Clin. Cancer Res.* 4:407–410.
- Tanaka, K., S. Iwamoto, G. Gon, T. Nohara, M. Iwamoto, and N. Tanigawa. 2000. Expression of survivin and its relationship to loss of apoptosis in breast carcinomas. *Clin. Cancer Res.* 6:127–134.
- Wang, F., V.M. Weaver, O.W. Petersen, C.A. Larabell, S. Dedhar, P. Briand, R. Lupu, and M.J. Bissell. 1998. Reciprocal interactions between $\beta 1$ -integrin and epidermal growth factor receptor in three-dimensional basement membrane breast cultures: a different perspective in epithelial biology. *Proc. Natl. Acad. Sci. USA*. 95:14821–14826.
- Wasserberg, N., S. Morgenstern, J. Schachter, E. Fenig, S. Lelcuk, and H. Gutman. 2002. Risk factors for lymph node metastases in breast ductal carcinoma in situ with minimal invasive component. *Arch. Surg.* 137:1249–1252.
- Weaver, V.M., A.H. Fischer, O.W. Peterson, and M.J. Bissell. 1996. The importance of the microenvironment in breast cancer progression: recapitulation of mammary tumorigenesis using a unique human mammary epithelial cell model and a three-dimensional culture assay. *Biochem. Cell Biol.* 74:833–851.
- Weaver, V.M., O.W. Petersen, F. Wang, C.A. Larabell, P. Briand, C. Damsky, and M.J. Bissell. 1997. Reversion of the malignant phenotype of human breast cells in three-dimensional culture and in vivo by integrin blocking antibodies. *J. Cell Biol.* 137:231–245.
- Weaver, V.M., S. Lelievre, J.N. Lakins, M.A. Chrenek, J.C. Jones, F. Giancotti, Z. Werb, and M.J. Bissell. 2002. $\beta 4$ integrin-dependent formation of polarized three-dimensional architecture confers resistance to apoptosis in normal and malignant mammary epithelium. *Cancer Cell*. 2:205–216.
- Wong, C.W., A. Lee, L. Shientag, J. Yu, Y. Dong, G. Kao, A.B. Al-Mehdi, E.J. Bernhard, and R.J. Muschel. 2001. Apoptosis: an early event in metastatic inefficiency. *Cancer Res.* 61:333–338.
- Wouters, B.G., M. Koritzinsky, R.K. Chiu, J. Theys, J. Buijsen, and P. Lambin. 2003. Modulation of cell death in the tumor microenvironment. *Semin. Radiat. Oncol.* 13:31–41.